New Astronomy 27 (2014) 81–94

Contents lists available at ScienceDirect

New Astronomy

journal homepage: www.elsevier.com/locate/newast

Magnetic activity and orbital period variation of the eclipsing binary KV Gem

Liyun Zhang [a,b,*], Qingfeng Pi [a,b], Yuangui Yang [c], Zhongmu Li [d]

[a] College of Science/Department of Physics & NAOC-GZU-Sponsored Center for Astronomy Research, Guizhou University, Guiyang 550025, PR China
[b] Key Laboratory for the Structure and Evolution of Celestial Objects, Chinese Academy of Sciences, Kunming 650011, PR China
[c] School of Physics and Electronic Information, Huaibei Normal University, Huaibei 235000, PR China
[d] Institute for Astronomy and History of Science and Technology, Dali University, Dali 671003, PR China

HIGHLIGHTS

- We present new CCD BVRI light curves of KV Gem in 2010 and 2011.
- Photometric solutions of KV Gem are obtained and starspot parameters are also derived.
- KV Gem exists a cyclic variation overlaying a continuous period decrease.
- This cyclic variation maybe caused by the light-time effect or magnetic cycle.

ARTICLE INFO

Article history:
Received 13 September 2011
Received in revised form 25 August 2013
Accepted 6 September 2013
Available online 21 September 2013
Communicated by W. Soon

Keywords:
Stars
Contact – binaries
Eclipsing – stars
Individual KV Gem – stars
Period variation

ABSTRACT

This paper presents new CCD *BVRI* light curves of **a** neglected eclipsing binary KV Gem. Our new light curves were obtained in 2010 and 2011 at the Xinglong station of the National Astronomical Observatories, China. By analyzing all available light minimum times, we derived an update ephemeris and found there existed a cyclic variation overlaying a continuous period decrease. This kind of cyclic variation may probably be attributed to the light-time effect via the presence of an unseen third body or magnetic activity cycle. The long-term period decrease suggests that KV Gem is undergoing a mass transfer from the secondary component to the primary component at a rate of $3.4(0.3) \times (10^{-7}$ $M_{\odot}$/year for period decrease and a third body (10.3 ± 0.2 years), and $5.5(0.6) \times 10^{-7}$ $M_{\odot}$/year for decrease and magnetic cycle (8.8 ± 0.1 years). By analyzing the light curves in 2011, photometric solutions and starspots parameters of the system are obtained using Wilson–Devinney program. Based on the photometric solution in 2011, we still could use the spot model to explain successfully our light curves in 2010 and three published light curves. Comparing the starspot longitudes and factors, KV Gem are variable on a long time scale of about years. For the data of KV Gem, the brightness vary with time around phases 0, 0.25, 0.5, and 0.75, which means that there is a possible photospheric active evolution. More data are needed to monitor to detect stellar cycle of KV Gem. For chromospheric activity of KV Gem, we found strong absorption in the observed H_{β}, H_{γ}, and Ca II H & K spectra, and no obvious emission.

1. Introduction

Near-contact binary is a key evolutionary stage for the formation and evolution of a close binary. They are very interesting targets, especially near contact eclipsing binary. By analyzing photometric light curves (LCs) and spectroscopic spectra, we could obtained orbital parameters of eclipsing binary, and discuss photospheric starspot and chromospheric activities. For many near contact eclipsing binaries, they display long-term variations (period increase or period decrease or/and period cyclic variation...) of orbital periods (Qian, 2002; Zhu and Qian, 2006; Hoffman et al., 2006; Coughlin et al., 2008). The long continuous period increase or decrease may result from mass transfer between components or stellar magnetic winds. For thermal relaxation oscillation models (Lucy, 1976; Flannery, 1976; Robertson and Eggleton, 1977; Kaluzny, 1985; Hilditch et al., 1988; Shaw, 1994; etc), the mass transfer might cause the weak-contact binary to evolve into either a deeper-contact configuration or a broken-contact configuration. Recently, a new theory of contact binary formation come into being (Stępień, 2006; Eker et al., 2007) based on magnetized stellar wind. They present a new method for evolution of contact binaries from detached systems. Sometime the variation of the orbital period show periodicity (Hoffman et al., 2006; etc). The physical mechanism for orbital period cyclic variation might be a third companion,

* Corresponding author at: College of Science/Department of Physics & NAOC-GZU-Sponsored Center for Astronomy Research, Guizhou University, Guiyang 550025, PR China. Tel.: +86 851 362 7662; fax: +86 851 362 7662.
E-mail address: liy_zhang@hotmail.com (L. Zhang).

1384-1076/$ - see front matter © 2013 Elsevier B.V. All rights reserved.
http://dx.doi.org/10.1016/j.newast.2013.09.002

Table 1
The observational log.

Star name or ID	coordinate(Ra;Dec 2000)	Mag_B	Mag_V	Mag_J	Mag_H	References
KV Gem(GSC01330-01213)	06:47:12.6;15:43:35	12.4	12.16	10.663	10.355	1,2,3
TYC 1330-119-1	06:47:00.8;15:46:06	12.03	11.78			3
GSC01330-00101	06:47:05.4;15:43:33	13.6	12.9	12	11.8	4

Reference: 1. Samus et al. (2003); 2. Gettel et al. (2006); 3. Hog et al. (2000); 4. Cutri et al. (2003).

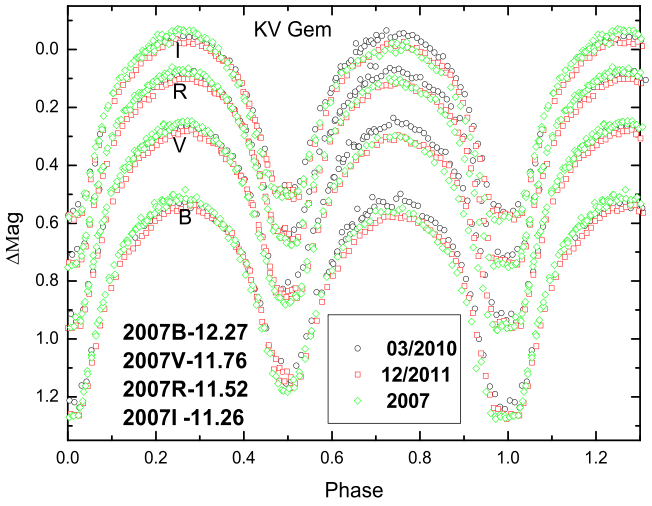

Fig. 1. B, V, R, and I light curves of KV Gem. Squares (□) indicate Dec. 2011, circles (○)-Mar 2010 and Diamond (2007 – data published by Coughlin (2010).

Table 2
Our new times of minimum of KV Gem.

HJD	Error	Filter	Type
2455282.12891	0.00075	B	primary
2455282.12984	0.00031	V	primary
2455282.12956	0.00039	R	primary
2455282.12924	0.00031	I	primary
2455284.10265	0.00035	B	Secondary
2455284.10210	0.00034	V	Secondary
2455284.10226	0.00054	R	Secondary
2455284.10201	0.00069	I	Secondary
2455910.07940	0.0002	B	Secondary
2455910.07950	0.0002	V	Secondary
2455910.07940	0.0001	R	Secondary
2455910.07945	0.0001	I	Secondary
2455910.25770	0.0002	B	primary
2455910.2579	0.0002	V	primary
2455910.25780	0.0003	R	primary
2455910.25750	0.0002	I	primary

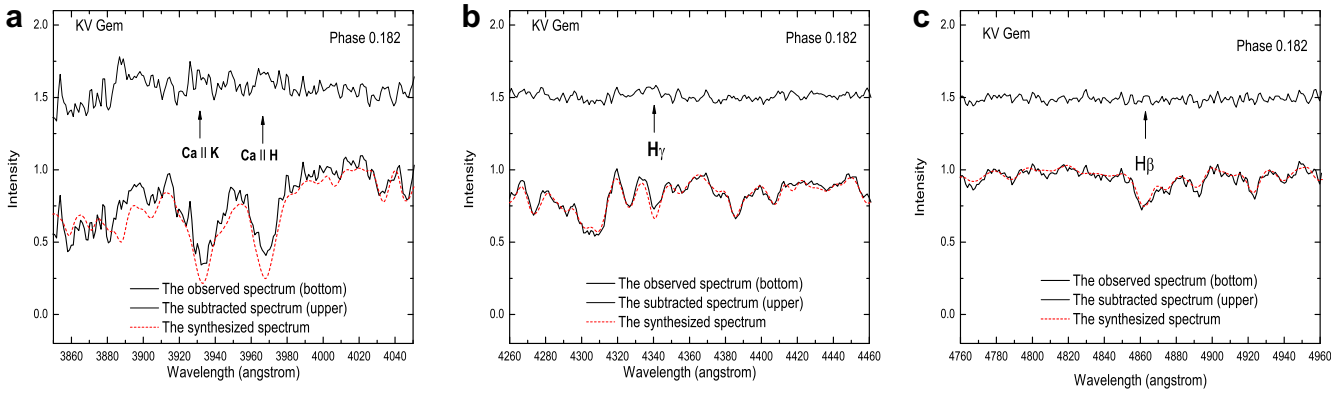

Fig. 2. The observed, synthesized, and subtracted spectra for the Ca II H & K, H beta and H gamma lines of KV Gem. The dotted lines represent the synthesized spectra and the upper spectra are the subtracted spectra.

or magnetic cycle (Applegate, 1992; Lanza et al., 1998; etc). KV Gem is an interesting eclipsing binary to discuss photospheric and chromospheric activity, and period variation.

KV Gem was first designated as a variable star by Kukarkin et al. (1968). Later, it was classified as the shortest period RR Lyrae (p = 0.2185467), by the general catalogue of variable star (Kholopov et al., 1985). In 1991, Schmidt (1991) found that KV Gem seemed to be an eclipsing binary with period of 0.43713 days. Recently, it was definitively re-confirmed as an eclipsing binary based on the first accurate multi-color light curves, and refined the period as 0.358 days (Coughlin, 2010). They also suggest that there might be a quasi-sinusoidal trend in the O–C diagram. At the same time, they also derived the orbital and spot parameters of KV Gem by modeling the light curve.

In this paper, we present our new B, V, R, and I LCs of KV Gem and analyze them using the 2003 version of Wilson–Devinney (WD) code (Wilson and Devinney, 1971; Wilson, 1990, 1994; Wilson and Van Hamme, 2004). Moreover, we accumulated all available times of light minimum and discussed the period change in detail for the first time.

2. New CCD photometric and spectroscopic observations of KV Gem

The new photometric observations were made during two observational runs (Mar. 26 and 28, 2010, and Dec. 14, 2011) with the 85-cm telescope of Xinglong station of the National Astronomical Observatories of China (NAOC). The photometer was equipped with a 1024 × 1024 pixel CCD and the standard Johnson–Cousin–Bessell *BVRI* filters (Zhou et al., 2009). The observations of KV Gem were made in B, V, R, and I passbands, and all observed CCD images were reduced by means of the IRAF[1] Package in the

[1] IRAF is distributed by the National Optical Astronomy Observatories, which are operated by the Association of Universities for Research in Astronomy, Inc., under cooperative agreement with the National Science Foundation.

Table 3
The minimum times of KV Gem.

HJD(2400000,+)	Error	Cycle	Method	Min	Weight	$(O-C)_1$	$(O-C)_2$	$(O-C)_2$	Reference
50839.3303	0.0028	−4000.0	ccd	I	10	0.0011	0.00066	0.00295	1
50849.3680	0.0028	−3972.0	ccd	I	10	0.0002	−0.00020	0.00199	1
51193.3688	0.0016	−3012.5	ccd	II	10	−0.0013	−0.00028	−0.00099	2
51481.4279	0.0013	−2209.0	ccd	I	1	−0.0149	−0.01336	−0.01512	2
51484.4879	0.0013	−2200.5	ccd	II	10	−0.0024	−0.00086	−0.00262	2
51841.5778	0.0033	−1204.5	ccd	II	10	−0.0008	0.00058	−0.00114	3
51876.5337	0.0021	−1107.0	ccd	I	10	−0.0008	0.00053	−0.00114	3
51909.5178	0.0023	−1015.0	ccd	I	10	−0.0008	0.00048	−0.00114	3
51923.3218	0.0035	−976.5	ccd	II	10	0.0001	0.00136	−0.00024	4
51924.3957	0.0020	−973.5	ccd	II	10	−0.0015	−0.00024	−0.00184	5
51924.5744	0.0014	−973.0	ccd	I	10	−0.0021	−0.00084	−0.00244	5
51965.2690	0.0065	−859.5	ccd	II	10	0.0002	0.00139	−0.00014	5
51965.4456	0.0054	−859.0	ccd	I	10	−0.0025	−0.00131	−0.00284	5
52234.6979	0.0020	−108.0	ccd	I	10	−0.0005	0.00016	−0.00091	5
52280.4100	0.0005	19.5	ccd	II	10	0.0000	0.00056	−0.00044	6
52280.5895	0.0007	20.0	ccd	I	10	0.0003	0.00086	−0.00014	6
52621.9230		972.0	ccd	I	1	0.0204	0.02016	0.01951	7
52683.3904	0.0041	1143.5	ccd	II	10	0.0012	0.00082	0.00019	5
52690.3810		1163.0	pe	I	10	0.0006	0.00020	−0.00042	8
52690.5576		1163.5	pe	II	10	−0.0020	−0.00240	−0.00302	8
52691.2757		1165.5	pe	II	10	−0.0010	−0.00140	−0.00202	8
52691.4562		1166.0	pe	I	10	0.0003	−0.00010	−0.00072	8
52692.3516		1168.5	pe	II	10	−0.0006	−0.00100	−0.00163	8
52692.5310		1169.0	pe	I	10	−0.0005	−0.00090	−0.00153	8
52694.3242		1174.0	pe	I	10	0.0001	−0.00031	−0.00093	8
52694.5028		1174.5	pe	II	10	−0.0006	−0.00101	−0.00163	8
52696.4769	0.0028	1180.0	ccd	I	10	0.0017	0.00129	0.00067	5
52697.3727	0.0034	1182.5	ccd	II	10	0.0012	0.00078	0.00016	5
52707.4094	0.0006	1210.5	ccd	II	10	−0.0008	−0.00124	−0.00186	8
52716.3731	0.0009	1235.5	ccd	II	10	−0.0001	−0.00056	−0.00118	8
52721.3934	0.0003	1249.5	ccd	II	10	0.0009	0.00043	−0.00019	8
52722.2897	0.0017	1252.0	ccd	I	10	0.0009	0.00043	−0.00019	5
52722.4703	0.0021	1252.5	ccd	II	10	0.0022	0.00173	0.00111	9
52723.3657	0.0042	1255.0	ccd	I	10	0.0013	0.00082	0.00021	5
52734.3006	0.0035	1285.5	ccd	II	10	0.0013	0.00080	0.00018	5
52735.3752	0.0021	1288.5	ccd	II	10	0.0003	−0.00020	−0.00082	10
52982.5765	0.0072	1978.0	ccd	I	10	0.0004	−0.00065	−0.00130	10
52984.5488	0.0046	1983.5	ccd	II	10	0.0008	−0.00026	−0.00091	10
53007.4936	0.0009	2047.5	ccd	II	10	0.0002	−0.00090	−0.00157	10
53028.2880	0.0013	2105.5	ccd	II	10	0.0003	−0.00084	−0.00152	10
53055.3562	0.0009	2181.0	ccd	I	10	0.0000	−0.00120	−0.00188	10
53055.5348	0.0011	2181.5	ccd	II	10	−0.0006	−0.00180	−0.00248	10
53070.4141	0.0006	2223.0	ccd	I	10	0.0000	−0.00123	−0.00192	10
53081.3499	0.0006	2253.5	ccd	II	10	0.0009	−0.00035	−0.00105	10
53082.4263	0.0010	2256.5	ccd	II	10	0.0017	0.00045	−0.00025	10
53088.3412	0.0014	2273.0	ccd	I	10	0.0010	−0.00026	−0.00096	9
53096.4105	0.0028	2295.5	ccd	II	10	0.0035	0.00222	0.00152	9
53329.4482	0.0004	2945.5	ccd	II	10	0.0017	0.00004	−0.00077	11
53329.6271	0.0002	2946.0	ccd	I	10	0.0013	−0.00036	−0.00117	11
53387.5298	0.0014	3107.5	pe	II	10	0.0026	0.00087	0.00004	9
53407.4325	0.0084	3163.0	ccd	I	10	0.0073	0.00555	0.00471	9
53408.5014	0.0016	3166.0	ccd	I	10	0.0007	−0.00105	−0.00189	12
53409.3982	0.0050	3168.5	ccd	II	10	0.0012	−0.00056	−0.00139	9
53410.4736	0.0011	3171.5	ccd	II	10	0.0010	−0.00076	−0.00159	12
53422.6635	0.0003	3205.5	ccd	II	10	0.0011	−0.00067	−0.00151	13
53443.6365	0.0002	3264.0	ccd	I	10	0.0006	−0.00119	−0.00203	13
53451.3464	0.0002	3285.5	ccd	II	10	0.0023	0.00050	−0.00034	14
53465.3281	0.0001	3324.5	ccd	II	10	0.0016	−0.00021	−0.00105	14
53684.9216	0.0002	3937.0	ccd	I	10	0.0001	−0.00181	−0.00261	13
53700.8758	0.0001	3981.5	ccd	II	10	0.0001	−0.00181	−0.00260	13
53704.8198	0.0001	3992.5	ccd	II	10	0.0003	−0.00161	−0.00239	15
53715.3974	0.0004	4022.0	ccd	I	10	0.0015	−0.00041	−0.00119	14
53715.5759	0.0004	4022.5	ccd	II	10	0.0007	−0.00121	−0.00198	14
53728.8410	0.0001	4059.5	ccd	II	10	0.0005	−0.00140	−0.00217	13
53745.5109	0.0033	4106.0	ccd	I	10	−0.0009	−0.00280	−0.00356	12
53752.5055	0.0091	4125.5	ccd	II	10	0.0025	0.00060	−0.00015	12
53760.3910	0.0001	4147.5	ccd	II	10	0.0005	−0.00139	−0.00214	12
53760.5708	0.0002	4148.0	ccd	I	10	0.0011	−0.00079	−0.00154	12
53791.4033	0.0038	4234.0	ccd	I	10	0.0007	−0.00117	−0.00190	4
54092.3841	0.0012	5073.5	ccd	II	10	0.0019	0.00059	0.00016	16
54092.5623	0.0017	5074.0	ccd	I	10	0.0008	−0.00051	−0.00094	16
54150.2843	0.0002	5235.0	pe	I	10	0.0007	−0.00039	−0.00077	17
54158.5340	0.0009	5258.0	ccd	I	10	0.0044	0.00334	0.00297	18
54158.7115	0.0026	5258.5	ccd	II	10	0.0027	0.00164	0.00127	18

(*continued on next page*)

Table 3 (*continued*)

HJD(2400000,+)	Error	Cycle	Method	Min	Weight	$(O-C)_1$	$(O-C)_2$	$(O-C)_2$	Reference
54159.6059	0.0002	5261.0	ccd	I	10	0.0008	−0.00026	−0.00063	18
54159.7875	0.0008	5261.5	ccd	II	10	0.0031	0.00205	0.00167	18
54405.3990	0.0004	5946.5	pe	II	1	0.0267	0.02714	0.02672	19
54454.3086	0.0004	6083.0	ccd	I	10	−0.0020	−0.00114	−0.00163	19
54454.4897	0.0006	6083.5	ccd	II	10	−0.0001	0.00076	0.00027	19
54505.3990	0.0004	6225.5	ccd	II	10	−0.0010	0.00034	−0.00025	19
54507.3696	0.0003	6231.0	ccd	I	10	−0.0023	−0.00094	−0.00154	19
54509.3437	0.0005	6236.5	ccd	II	10	0.0000	0.00138	0.00078	19
54509.5203	0.0010	6237.0	ccd	I	10	−0.0027	−0.00132	−0.00192	19
54515.4374	0.0005	6253.5	ccd	II	10	−0.0012	0.00024	−0.00037	19
54516.3333	0.0005	6256.0	ccd	I	10	−0.0016	−0.00015	−0.00077	19
54516.5128	0.0007	6256.5	ccd	II	10	−0.0014	0.00005	−0.00057	19
54520.4566	0.0007	6267.5	ccd	II	10	−0.0013	0.00019	−0.00044	19
54531.3915	0.0005	6298.0	ccd	I	10	−0.0014	0.00020	−0.00045	19
54809.6021	0.0004	7074.0	ccd	I	10	−0.0042	0.00053	−0.00091	20
54843.3029	0.0014	7168.0	ccd	I	10	−0.0045	0.00061	−0.00091	21
54843.4809	0.0005	7168.5	ccd	II	10	−0.0057	−0.00059	−0.00211	21
54856.3877	0.0005	7204.5	ccd	II	10	−0.0057	−0.00045	−0.00199	21
54884.7087	0.0007	7283.5	ccd	II	10	−0.0080	−0.00244	−0.00403	22
54910.3586	0.0001	7355.0	ccd	I	1	0.0075	0.01333	0.01170	23
55201.2838	0.0010	8166.5	ccd	II	10	−0.0082	0.00028	−0.00133	24
55244.3074	0.0019	8286.5	ccd	II	10	−0.0073	0.00151	−0.00005	24
55249.3253	0.0003	8300.5	ccd	II	10	−0.0087	0.00015	−0.00140	25
55259.7210	0.0004	8329.5	ccd	II	10	−0.0101	−0.00117	−0.00271	26
55282.1294	0.0004	8392.0	ccd	I	10	−0.0094	−0.00031	−0.00181	27
55284.1023	0.0004	8397.5	ccd	II	10	−0.0084	0.00071	−0.00079	27
55910.0795	0.0001	10143.5	ccd	II	10	−0.0113	0.00147	0.00124	27
55910.2577	0.0020	10144.0	ccd	I	10	−0.0123	0.00047	0.00024	27
55544.9242	0.0004	9125.0	ccd	I	10	−0.0115	−0.00069	−0.00168	28
55578.2670	0.0003	9218.0	ccd	I	10	−0.0113	−0.00029	−0.00122	29
55578.4478		9218.5	ccd	II	10	−0.0097	0.00131	0.00038	30
55578.6254		9219.0	ccd	I	10	−0.0114	−0.00039	−0.00131	30
50080.4327		−6116.5	ccd	II	0	−0.0838	−0.08300	−0.07509	31
50463.5013		−5048.5	ccd	II	0	0.0828	0.08196	0.08753	32
51165.4878		−3090.5	ccd	II	0	0.0825	0.08343	0.08289	33
52359.3696		239.5	ccd	II	0	0.0847	0.08508	0.08419	34
30428.3500		−60931.0	pg	I	0	0.0596	0.50717	0.79376	35
31031.5800		−59248.5	pg	II	0	0.0756	0.49686	0.76973	35
38385.4800		−38736.5	pg	II	0	−0.0359	0.14330	0.26591	35
38816.4000		−37534.5	pg	II	0	−0.0598	0.10719	0.22484	35
39905.2600		−34497.5	pg	II	0	−0.0323	0.11183	0.21177	35
39942.4000		−34394.0	pg	I	0	0.0006	0.14407	0.24325	35
49048.4460		−8995.0	vis	I	0	−0.0638	−0.05456	−0.04373	36
50515.4023		−4903.5	vis	II	0	−0.0019	−0.00283	0.00236	37
51195.5199		−3006.5	vis	II	0	−0.0013	−0.00027	−0.00100	2
51237.4690		−2889.5	vis	II	0	0.0007	0.00185	0.00089	2
51193.5493		−3012.0	vis	I	0	0.0000	0.00102	0.00031	2
51518.5512		−2105.5	vis	II	0	0.0013	0.00286	0.00105	2
51550.2765		−2017.0	vis	I	0	−0.0026	−0.00103	−0.00287	3
51555.4767		−2002.5	vis	II	0	−0.0010	0.00057	−0.00128	38
51569.2791		−1964.0	vis	I	0	−0.0017	−0.00013	−0.00198	3
51569.4579		−1963.5	vis	II	0	−0.0022	−0.00063	−0.00248	3
51572.3272		−1955.5	vis	II	0	−0.0010	0.00057	−0.00129	38
51576.4544		−1944.0	vis	I	0	0.0031	0.00467	0.00281	3

1.Šafář and Zejda (2000); 2. Šafář and Zejda (2002); 3.Zeijda (2002); 4. Brát et al. (2007); 5. Zejda (2004); 6. Agerer and Hübscher (2002); 7. Paschke Anton; 8. Agerer and Hübscher J (2003); 9. Hübscher et al. (2005); 10. Hübscher (2005); 11. Zejda et al. (2006); 12. Hübscher et al. (2006); 13. Dvorak (2006); 14. Zejda et al. (2006); 15. Nelson 2006; 16. Hübscher and Walter (2007); 17. Hübscher (2007); 18. Coughlin (2010); 19. Hübscher et al. (2009); 20. Hübscher et al. (2009b); 21. Hübscher et al. (2010a); 22. Diethelm (2009); 23. Hübscher et al. (2010b); 24. Hübscher and Monninger (2011); 25. Smelcer ; 26. Diethelm (2010); 27. present paper; 28. Diethelm (2011); 29. Brát et al. (2011); 30. Hübscher (2011); 31. Agerer and Hübscher (1996); 32. Agerer and Hübscher (1998) ; 33 Agerer et al. (1999); 34. Achterberg Herbe (2003); 35. Meinunger; 36. Hübscher (1994); 37. Brat; 38. Safar Jan; We collected the minima from <http://var2.astro.cz/EN>/(Paschke and Brat (2006)) I: the primary minima; II: the secondary minima.

standard fashion. The magnitude values of KV Gem, the comparison, and the check star were determined using the Apphot sub-package of IRAF. The parameters of these objects are listed in Table 1. For our observations, the phases of data points were calculated using our new linear ephemeris. The light curves are displayed in Fig. 1, where Δ Mag represents the differential magnitude between KV Gem and the comparison. The errors of magnitude are about 0.01 mag in B, V, R, and I.

Our spectroscopic observations of KV Gem (Fig. 2) were carried out with the OMR spectrograph of the 2.16 m telescope at the Xinglong station of NAOC in 2012. The OMR spectrograph centered at about 4280 Å with a reciprocal dispersion of 1.03 Å / pixel and wavelength range of 3700–4960 Å (Fang et al., 2010). The observational exposure time is 20 min. The corresponding signal to noise (S/N) was about 30. We also obtained a high S/N spectrum of the HD 102870 (F9 V), HR 4277 (G0 V), HD 68256 (G5 V), HD 127334 (G5 V), HD 153226 (K0 V), HR 1614 (K3 V), HR 3545 (K1 IV); M dwarf HR 2458 (M1 V), HR 2216 (M3 III) . . .for use as inactive templates. Reduction of the spectra was performed using IRAF packages and involved bias subtraction, flat-fielding, cosmic-ray removal, one dimensional spectrum extraction and wavelength calibration.

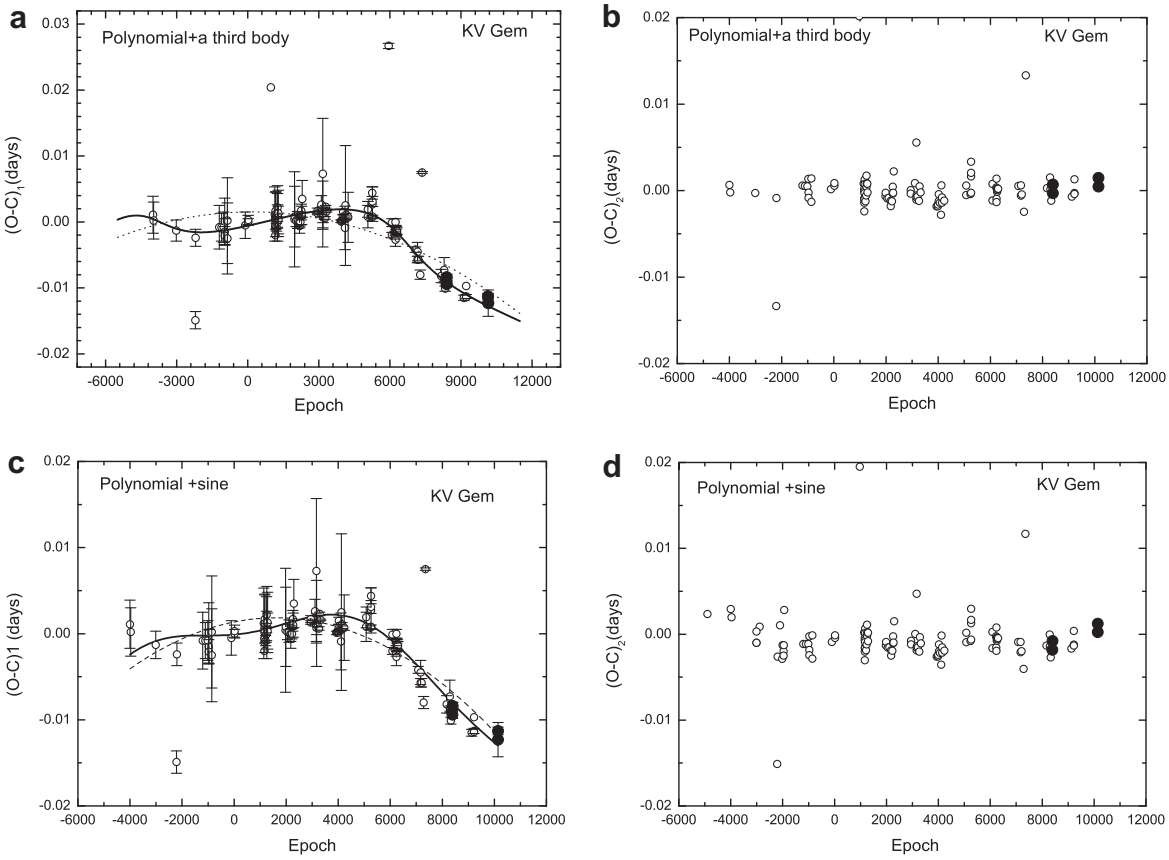

Fig. 3. Left: The (O–C) diagram of KV Gem. The $(O-C)_1$ values were computed by using a newly determined linear ephemeris (Eq.(1). The dashed line represents the quadratic fit; the solid line represents quadratic fit superimposed on a cyclic variation (a third body or magnetic cycle). Right: The corresponding residuals $(O-C)_2$ of KV Gem. The solid points represent our new times of minima.

Table 4
Parameters of the assumed third body for the eclipsing binary KV Gem.

Parameters	Values
A(days)	0.0029(2)
P_3(yr)	10.3(2)
e	0.38(3)
omega(radians)	2.84(8)
T_P(HJD)	2454613.3(53.9)
a_12sini(AU)	0.54(3)
K_RV(Km s^-1)	1.6(2)
f(m)(Msun)	0.0015(3)

3. Orbital Period Variation for KV Gem

From our observations, the times of minimum for KV Gem were obtained using the method of Kwee and van Woerden (1956) with the polynomial fitting and the interpolation method by the program (Nelson, 2007). The individual minimum of BVRI bands, together with their errors are listed in Table 2. It would be very helpful to asses any possible wavelength dependence on O–C variations due to spots in the future. The average values of the time of minima of the different bands are used when discussing period variations. To discuss periodic variation, we compiled all available light minima, some of which were compiled at the Eclipsing Binaries Minima Database (available at http://var2.astro.cz/EN/). All the light minimum timings with their errors of KV Gem are listed in columns (1) and (2) in Table 3. The Epoch values of all data (column (3) of the Table 3) were based on the previous linear ephemeris $Min.I = HJD2450839.3262(\pm0.0002) + 0^d.35852290$

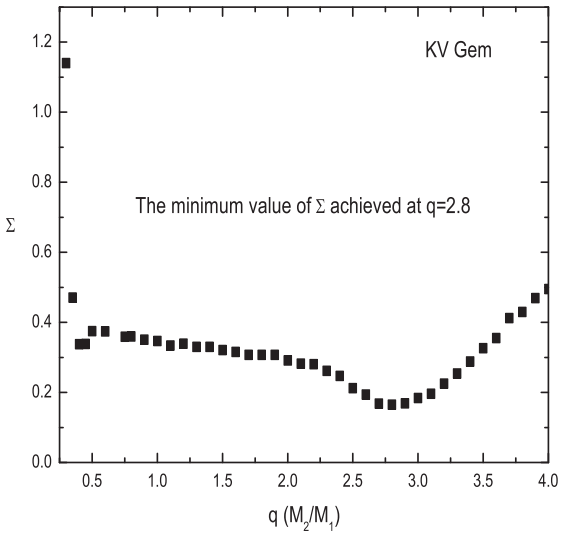

Fig. 4. The relation between the sum of the squares of the residuals and the mass ratio q of KV Gem.

(±0.0000006) E given by Coughlin (2010). The column (4) of the Table 3 are the observational methods, where "CCD" to charge-coupled devices, "pe" to photoelectric data, "pg" refers to photographic data, and "vi" to visual observations, . The collected minimum timings provide some important new information about the period change of KV Gem. Using the linear least-squares method, an update linear ephemeris is given by Eq. (1):

Table 5
The orbital result derived by Coughlin (2010) and our results of LC analysis for KV Gem in 2011.

Element	Coughlin 2007	2011	2011	2011	2011
type	case3	case1	case2	case3	case4
T1(K)	6000a	6000a	6000a	6000a	6000a
q	2.87	2.800+/−0.005	2.800+/−0.007	2.800+/−0.008	2.800+/−0.005
i(degree)	89.3	88.205+/−0.025	88.807+/−0.249	88.613+/−0.231	88.741+/−0.021
T2(K)	5799	5556+/−5	5672+/−6	5579+/−5	5695+/−5
Omega_1,2	–	6.245+/−0.006	6.260+/−0.009	6.208+/−0.007	6.245+/−0.005
(L1/(L1+L2))_B	–	0.3920+/−0.0009	0.3611+/−0.0009	0.3876+/−0.0009	0.3559+/−0.0009
(L1/(L1+L2))_V	–	0.3618+/−0.0007	0.3396+/−0.0007	0.3591+/−0.0007	0.3360+/−0.0007
(L1/(L1+L2))_R	–	0.3460+/−0.0006	0.3282+/−0.0006	0.3442+/−0.0006	0.3255+/−0.0006
(L1/(L1+L2))_I	–	0.3344+/−0.0005	0.3199+/−0.0005	0.3332+/−0.0005	0.3178+/−0.0005
r1_(pole)	–	0.2817+/−0.0006	0.2806+/−0.0008	0.2845+/−0.0007	0.2817+/−0.0005
r1_(side)	–	0.2946+/−0.0007	0.2933+/−0.0010	0.2979+/−0.0008	0.2946+/−0.0006
r1_(back)	–	0.3332+/−0.0013	0.3310+/−0.0018	0.3390+/−0.0016	0.3332+/−0.0011
r1_(average)	0.291	0.3032+/−0.0009	0.3016+/−0.0012	0.3071+/−0.0010	0.3031+/−0.0007
r2_(pole)	0.474	0.4492+/−0.0005	0.4482+/−0.0006	0.4518+/−0.0005	0.4492+/−0.0004
r2_(side)	0.474	0.4826+/−0.0006	0.4812+/−0.0009	0.4861+/−0.0007	0.4826+/−0.0005
r2_(back)	0.474	0.5114+/−0.0008	0.5096+/−0.0011	0.5159+/−0.0009	0.5114+/−0.0007
r2_(average)	0.474	0.4811+/−0.0007	0.4797+/−0.0009	0.4846+/−0.0007	0.4811+/−0.0005
Latitude_spot1(degree)	124.2	90a	90a	90a	90a
Longitude_spot1(degree)	152.7	29.15 +/−12.15	33.0+/−0.4	37.53+/−0.8	33.0+/−0.5
Radius_spot1(degree)	28.1	17.47+/−6.78	11.2+/−0.4	19.4 +/−0.3	11.9+/−0.3
Temperature_spot1(K)	4068	4984+/−201	3773+/−285	4984 +/−48	3680+/−305
Latitude_spot2(degree)	155.8	90a	90a	90a	90a
Longitude_spot2(degree)	187	238.22+/−0.63	247.33+/−0.85	255.45+/−0.2	259.4+/−0.3
Radius_spot2(degree)	37.4	21.41+/−0.63	22.57+/−0.29	17.4+/−0.1	14.7+/−0.2
Temperature_spot2(K)	3688	4874+/−102	4888+/−36	4580+/−38	4371+/−55
Spot factor	–	1.11%	1.22%	1.33%	1.33%
The residuals	–	0.05958	0.0546	0.06378	0.0546

Parameters not adjusted in the solution are denoted by a mark "a".
Case1: spot1 and spot2 on the primary.
Case2: spot1 on the secondary and spot2 on the primary.
Case3: spot1 on the primary and spot2 on the secondary.
Case4: spot1 and spot2 on the secondary.

$$Min.I = HJD2452273.4188(\pm 0.0002) + 0^d.3585224(\pm 0.0000001)E \quad (1)$$

The O–C values of the eclipsing timings show a downward parabolic curve with a possible oscillation (Fig. 3), which indicate that there exists a cyclic variation overlaying a continuous period decrease. We used two methods – quadratic ephemeris + the light time effect (LITE) or polynomial + sine function to fit the minima. The light time effect and sine function respond to a third body and magnetic cycle, respectively. A weighted nonlinear least-squares fitting are used. The weights 0, 2 and 10 were given to visual, photographic, and photoelectric and CCD observations. For some minimum with larger standard deviations (most of data are visual and pg observations.), I have to give the weight of 0 or 1 because the amplitude of the cyclic variation is very low and the errors of visual observation might be very larger. The periodic variation of minima was checked for periodicities in the range 0–15 years. The result of the quadratic ephemeris + LITE (Pribulla and Rucinski, 2006; Yang et al., 2007) are:

$$O-C = 0.0015(0.0001) + [4.0(9)\times 10^{-8}]E - [1.2(0.1)\times 10^{-10}]E^2 + \tau \quad (2)$$

and

$$\tau = \frac{a_{12}sini}{c}\left(\frac{1-e^2}{1+ecosv}sin(v+\omega) + esin\omega\right) \quad (3)$$

The semi-amplitude of the light-time effect is $A = a_{12}$sini/c, where a_{12} is the semiaxis of the eclipsing – pair orbit around the common center of mass with the third body and c is the velocity of light. The third body orbital parameter v, e, ω, and i are the true anomaly, eccentricity, longitude of the periastron, and inclination respectively, in Eq. (3). In order to simultaneously obtain these related parameters of Eq. (2) and (3), the Levenberg–Marquardt techniques were used (Press et al., 1992). The results are listed in Table 4. The calculated residuals $(O-C)_2$ are listed in column (8) of Table 3 and plotted in Fig. 3. The orbital period of the third body is $P_3 = 10.3(0.2)$ years. We also used a polynomial + sinusoidal function for fitting (O–C) which led to the following equation:

$$O-C = 0.0014(1) + [6.0(1.1)\times 10^{-7}]E - [1.9(0.2)\times 10^{-10}]E^2 + 0.0016(0.0002)\times sin(0.0007(0.0002)\times E + 1.9(0.1)) \quad (4)$$

The calculated residuals $(O-C)_2$ are listed in column (9) of Table 3 and plotted in Fig. 3. The sinusoidal term of the above equation reveals a periodic oscillation with an amplitude of $A = 0^d.0016(2)$ days. Using $T = 2\pi \times P/\omega$, where P denotes the orbital period of KV Gem in years and ω is the coefficient of E. The period of the oscillation T was calculated to be 8.8 ± 0.1 years.

4. Photometric and spectroscopic analysis of KV Gem

We will analyze the magnetic activities, and photometric solution of KV Gem in this section.

4.1. The chromospheric activity analysis

The CaII H & K, H_β, and H_γ lines are very useful diagnostic indicators of chromospheric activity for late-type stars (Montes et al., 1997; Gunn and Doyle, 1997; Montes et al., 2004; Zhang, 2011; etc.). Our normalized spectra of KV Gem was analyzed by the spectral subtraction technique using the program STARMOD (Barden, 1985; Montes et al., 1995). In this method, the synthesized spectra is constructed from artificially rotationally broadened, radial-velocity shifted, and weighted spectra of two inactive stars with the same spectral type and luminosity class similar to two components of the active system. The intensity weights (0.4/0.6) for spectral subtraction have been obtained from photometric light curve

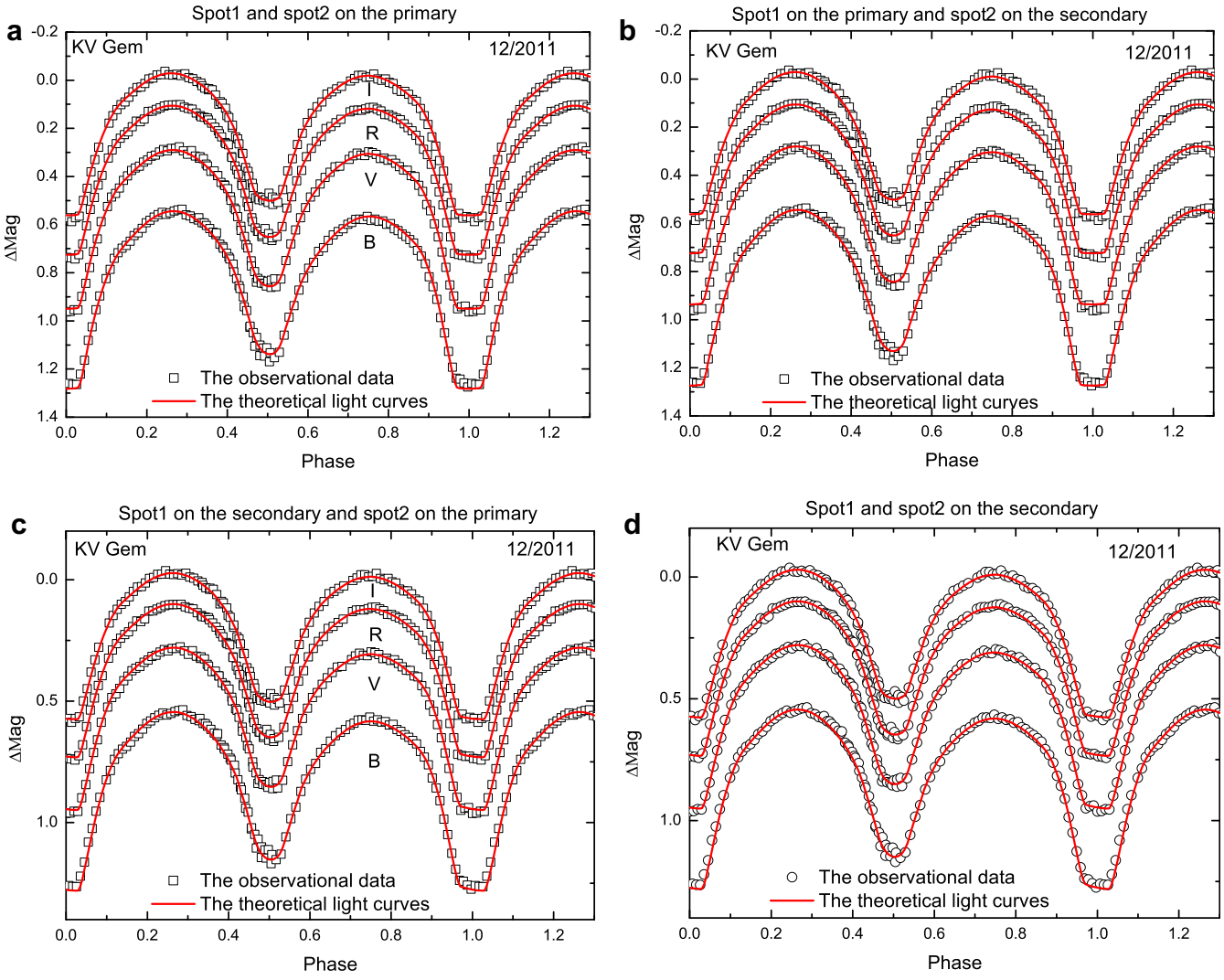

Fig. 5. The observational and theoretical light curves of KV Gem in 2011. The points and solid lines represent the observational and theoretical light curves, respectively.

modeling. This method was also used for discussing the chromospheric activity of other eclipsing binary ER Vul by Gunn and Doyle (1997). By comparison, we find that two inactive stars HD 102870 (F9 V) and HR 1614 (K3 V) are much better templates for KV Gem. The synthesized and subtracted spectra (the observed spectra minus the synthesized one) are shown in Fig. 2. Because our spectra are middle-resolution spectra, and KV Gem is a short period eclipsing binary, the spectra of the primary and secondary components are strongly blended. As can be seen from Fig. 2, we found strong absorption in the observed H_β and H_γ lines, and Ca II H & K spectra, and no obvious emission in the subtracted spectra. It is very difficult to tell which the primary or secondary component are active.

4.2. Photometric analysis

Because our data obtained in 2011 have high time resolution and full phase coverage, photometric solution of KV Gem might be obtained using the 2003 version of the Wilson–Devinney program (Wilson and Devinney, 1971, Wilson & Devinney 1979, Wilson, 1990, 1994; Wilson and Van Hamme, 2004, etc). Then, we will try to explain separately other four light curves (including the light curves published by Schmidt (1991) and Coughlin (2010), and All sky automated survey (ASAS) data (Pojmanski, 2002)) based on our photometric solutions in 2011.

4.2.1. Analysis of the light curves in December 2011

Individual points in B, V, R and I bands are used directly for photometric analysis, and the four LCs are simultaneously solved. Because of having no simultaneous high-resolution spectroscopic observations, we are not able to tell whether spots are located on the primary or secondary components. Therefore, we have performed four solutions (case1: spot1 (phase about 0.15) and spot2 (phase about 0.75) on the primary, case2: spot1 on the secondary and spot2 on the primary, case3: spot1 on the primary and spot2 on the secondary, case4: spot1 and spot2 on the secondary).

For our photometric solutions, we assumed synchronous rotation and zero eccentricity of KV Gem. Simple treatment is used to compute the reflect effect, and the linear limb-darkening law was used to compute the limb-darkening effect. The bolometric albedo $A_1 = A_2 = 0.5$ (Rucinski, 1973), the limb-darkening coefficients $x_{1B} = 0.705$ $x_{2B} = 0.742$, $x_{1V} = 0.575$ $x_{2V} = 0.608$, $x_{1R} = 0.475$ $x_{2R} = 0.503$, $x_{1I} = 0.389$ $x_{2I} = 0.413$ (Van Hamme, 1993), and the gravity-darkening coefficients $g_1 = g_2 = 0.32$ (Lucy, 1967) are set for the primary and secondary components. According to the color index J-H of 0.308 (This J-H color is not a dereddened color), the corresponding temperature of the primary (5961 ± 356 k) is calculated using the relation of effective temperature and the colors (Bessell and Brett, 1988; Cox, 2000) by the linear interpolation. The temperature of primary component refer to the assumed temperature (6000 K) in the paper by

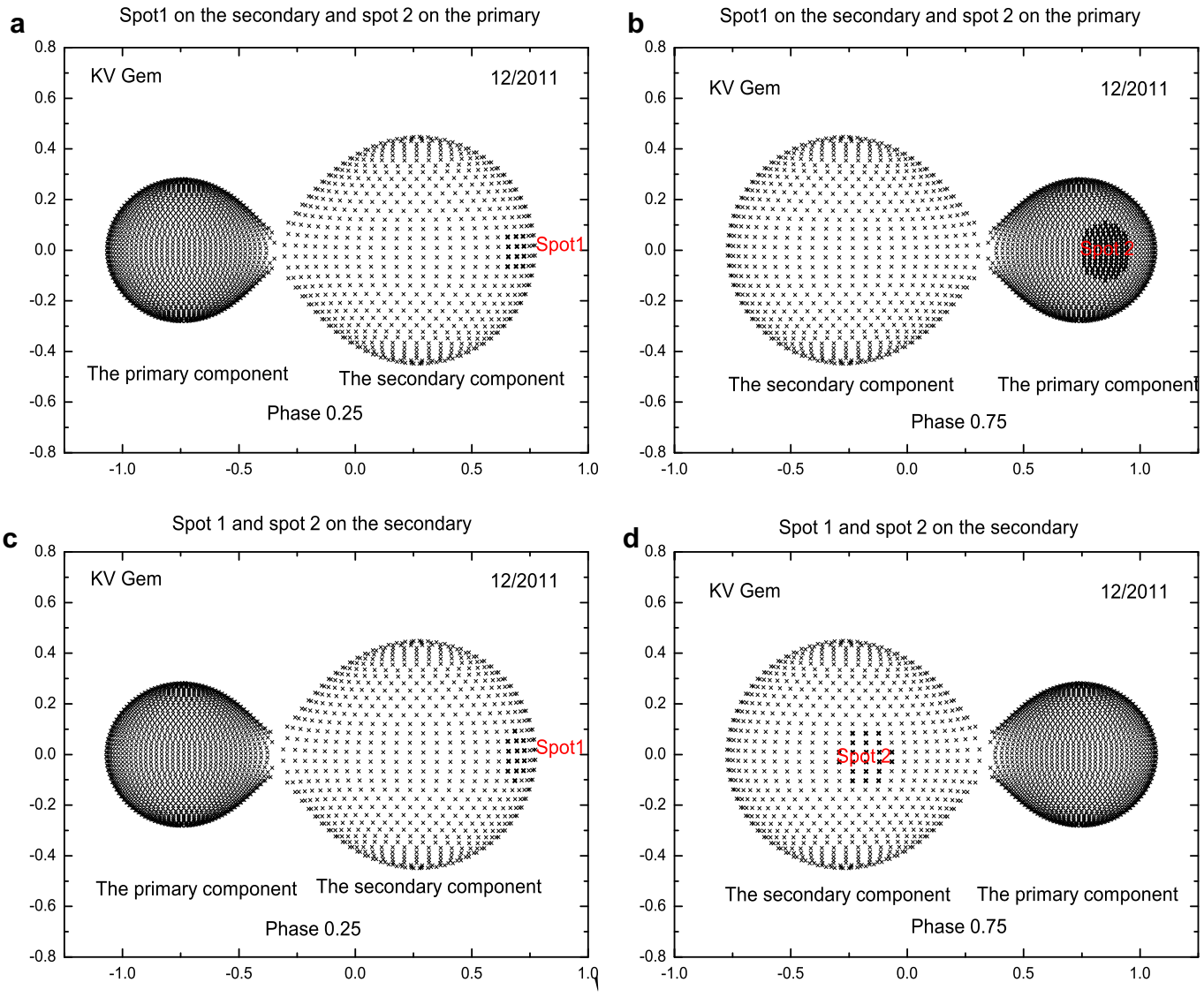

Fig. 6. Configurations of KV Gem of the results of case 2 and case 4 in phases 0.25 and 0.75 in Dec. 2011.

Coughlin (2010). Therefore, we fixed the temperature of primary as 6000 K. Since no spectroscopic mass ratios for system have been published, we needed to search for a reliable mass ratio $q = M_2/M_1$ (the secondary divided by the primary), via the differential correction program. For the purpose, the solutions for several assumed values of the mass ratio ($q = 0.3 - 3$) were obtained. For each assumed value of q, the light curves were solved based on mode 3 (contact mode) of Wilson and Devinney's DC Program.

When performing the differential correction (DC) calculation, the adjustable orbital parameters are the orbital inclination i, the temperature of the secondary T_2, the dimensionless potentials of the two components Ω_1 and Ω_2, and the monochromatic luminosity of the primary L_1 deriving from the approximate Kurucz atmosphere model option (Kurucz, 1993). The preliminary values of some orbital parameters (the orbital inclination, the temperature of the secondary component) are taken from photometric solution derived by Coughlin (2010). We separately adjusted the orbital parameters until these parameters coverage. The solutions were obtained for all assumed mass ratios. The details of the procedure of photometric solution is similar to that of photometric solutions of our previous works RT And (Zhang and Gu, 2007), DV Psc (Zhang et al., 2010a), GSC 3576-0170 (Zhang et al., 2010b), KQ Gem (Zhang, 2010) and V1034 Her (Zhang, 2012). The relation of the sum of weighted square deviation ($\sum_i (O-C)_i^2$) with mass ratio q is illustrated in Fig. 4, where the lowest value is $q = 2.8$. Therefore, it indicates that the most likely mass ratio appears to be approximately 2.8.

The details For the spot parameters, the latitude of the spot was assumed to be 90°, which means that its center is on the equator of the component. Therefore, we only adjust the remaining three parameters of the spot, the longitude of the spot center $longitude_{spot}$, the radius of the spot $radius_{spot}$ and temperature $factor_{spot}$. After a lot of runs, four photometric solutions of KV Gem were derived, which are listed in Table 5. The errors of photometric solutions are the formal errors on the WD differential correction program. They are underestimated and are not accurate errors because statistically rigorous errors cannot be obtained by WD program. The theoretical and observed light curves are shown in Fig. 5. The weighted sums of squares of residuals for case 2 and case 4 are smaller than those of case1 and case 3, so we conclude that the two case 2 and 4 are better for explaining the light curves. However, it is very difficult to tell which is better for them, because the weighted sum of squares of residuals of case 2 and case 4 are

very similar. Corresponding configurations of KV Gem in phases 0.25 and 0.75 are shown in Fig. 6. The period analysis indicated that the period oscillation may be caused by a third component, so we tied to adjust the parameters l_3 in the W-D code. However, the third light calculated by the program tended to zero.

4.2.2. Analysis of our light curves in March 2010 and other published light curves

Comparing the light curves with each other (Fig.1), there are some variations on the shapes. The above does indicate a starspot are variable on a long-time scale interval of several years.

As can be seen from Fig. 1, the LCs do not have sufficient phase coverage in 2010. Because the light curves show a O'Connell effect (Davidge and Milone, 1984; Kallrath and Milone, 2009). We try to obtain the reliable spot parameters on the base of our new photometric solutions of case 2 and case 4 of 2011. We fixed the orbital parameters and only adjusted the radius of starspot. After some runs, the results are obtained and listed in Table 6 and the weighted sum of squares of residuals based on the case 2 and case 4 are very similar. The theoretical LCs are shown in Fig. 7 and corresponding configurations of KV Gem are also shown in Fig. 7. Even though there is a small gap in 2010, the spot parameters might be real because the gap of our light curve is very small.

For the V and R light curves in 1991 published by Schmidt (1991), the light curves are symmetric and they might be no starspot or very small starspot on this season. Therefore, we adjust the luminosity of the primary L_1. After some runs, the results are obtained and listed in Table 6. The theoretical LCs are shown in Fig. 8. We also used the same method to explained the ASAS data of KV Gem (Pojmanski, 2002, 2003; Pojmanski et al., 2005). The results are also listed in Table 6 and the weighted sum of squares of residuals for the light curves of case 4 is smaller than that of case 2. The theoretical LCs are also shown in Fig. 8.

For the light curves published by Coughlin (2010) in 2007, there are two depressions in the phase ranges 0.45–0.5 (spot1) and 0.6–0.9 (spot2). For the spot 1, it might be located on the primary because most of the secondary component are eclipsed by the primary in phase 0.45–0.5. Therefore, there are only two possibility (Case1: spot1 and spot2 are on the primary, and Case 2: spot 1 on the primary and spot2 on the secondary.). To explain these light curves, we have to adjust some orbital parameters. After a lot of runs, two photometric solutions of KV Gem were derived. They are listed in Table 6, and the theoretical light curves are shown in Fig. 9. Corresponding configurations of KV Gem for these results in phases 0.5 and 0.75 are shown in Fig. 9. The weighted sum of squares of residuals of case 2 is smaller than that of case 1, so we conclude that the case 2 is better for explaining the distortion of the light curves in 2007. We found that many values of Case 2 are closer to the results of case 4 in 2011. In a word, the case 4 might be the best result of KV Gem.

5. Discussions and conclusions

Our new LCs and one spectra, and the period variation of KV Gem are included in present paper.

We obtained new precise photometric solution using the 2011 light curves. The orbital inclination (about 87°.7) is similar to that derived by Coughlin (2010). The contribution of the primary component of KV Gem to the total light is 0.36 in *B*, 0.34 in *V*, 0.33 in *R* and 0.32 in *I* band. The mass ratio of $q = 2.8$ is also similar to the result (2.87) derive by Coughlin (2010). The dimensionless potentials of the primary and secondary components are 6.26. The average relative radius is larger than the primary component (Table 5). Furthermore, the fact that the primary eclipse is flat-bottomed means that physically the primary, hotter star has to be physically smaller than the cooler secondary star. Our photometric result indicated that KV Gem is a contact binary system with a

Table 6
The results of other LC analysis for KV Gem.

Element	2010	2010	Schmidt (1991)	Schmidt (1991)	Coughlin2007	Coughlin2007	ASAS	ASAS
type	case2	case4	case2	case4	case1	case3	case2	case4
T1(K)	6000a	6000a	6000a	6000a	6000a	6000a	6000a	6000a
q	2.800a	2.800a	2.800a	2.800a	2.60+/-0.01	2.800a	2.800a	2.800a
i(degree)	88.807a	88.741a	88.807a	88.741a	88.662+/−0.502	88.741+/−0.167	88.807a	88.741a
T2(K)	5672a	5695a	5672a	5695a	5627+/−7~K	5679+/−7~K	5672a	5695a
Omega_1,2	6.260a	6.245a	6.260a	6.245a	5.869+/−0.012	6.105+/−0.012	6.260a	6.245a
(L1/(L1+L2))_B	0.3611a	0.3559+/−0.003	–	–	0.3944+/−0.0010	0.3672+/−0.0010	–	–
(L1/(L1+L2))_V	0.3396a	0.3360+/−0.004	0.340+/−0.001	0.336+/−0.001	0.3690+/−0.0009	0.3460+/−0.0009	0.340+/−0.001	0.336+/−0.001
(L1/(L1+L2))_R	0.3282a	0.3255+/−0.003	0.328+/−0.001	0.326+/−0.001	0.3556+/−0.0007	0.3347+/−0.0007	–	–
(L1/(L1+L2))_I	0.3199a	0.3178+/−0.003	–	–	0.3457+/−0.0013	0.3264+/−0.0006	–	–
r1_(pole)	–	–	–	–	0.2964+/−0.0016	0.2926+/−0.0004	–	–
r1_(side)	–	–	–	–	0.3116+/−0.0032	0.3078+/−0.0005	–	–
r1_(back)	–	–	–	–	0.3586+/−0.0020	0.3572+/−0.0011	–	–
r1_(average)	–	–	–	–	0.3222+/−0.0007	0.3192+/−0.0007	–	–
r2_(pole)	–	–	–	–	0.4519+/−0.0004	0.4593+/−0.0004	–	–
r2_(side)	–	–	–	–	0.4870+/−0.0006	0.4963+/−0.0006	–	–
r2_(back)	–	–	–	–	0.5199+/−0.0008	0.5294+/−0.0008	–	–
r2_(average)	–	–	–	–	0.4863+/−0.0006	0.4950+/−0.0006	–	–
Latitude_spot1(degree)	90a	90a	–	–	90a	90a	–	–
Longitude_spot1(degree)	33.0a	33.0a	–	–	129.6+/−1.3	171.1+/−12.9	–	–
Radius_spot1(degree)	8.6+/−0.3	10.3+/−0.1	–	–	12.0+/−0.5	7.0+/−3.5	–	–
Temperature_spot1(K)	3773a	3680a	–	–	5409+/−101	5823+/−166	–	–
Latitude_spot2(K)	–	–	–	–	90a	90a	–	–
Longitude_spot2(degree)	–	–	–	–	286.5+/−0.9	297.8+/−0.8	–	–
Radius_spot2(degree)	–	–	–	–	15+/−0.3	17.3+/−0.5	–	–
Temperature_spot2(K)	–	–	–	–	4741+/−45	4360a	–	–
Spot factor	0.30%	0.45%	0%	0%	1.20%	0.98%	0%	0%
The residuals	0.1083	0.1057	0.271	0.272	0.087	0.0792	0.763	0.76

Parameters not adjusted in the solution are denoted by a mark "a".
Case1: spot1 and spot2 on the primary.
Case2: spot1 on the secondary and spot2 on the primary.
Case3: spot1 on the primary and spot2 on the secondary.
Case4: spot1 and spot2 on the secondary.

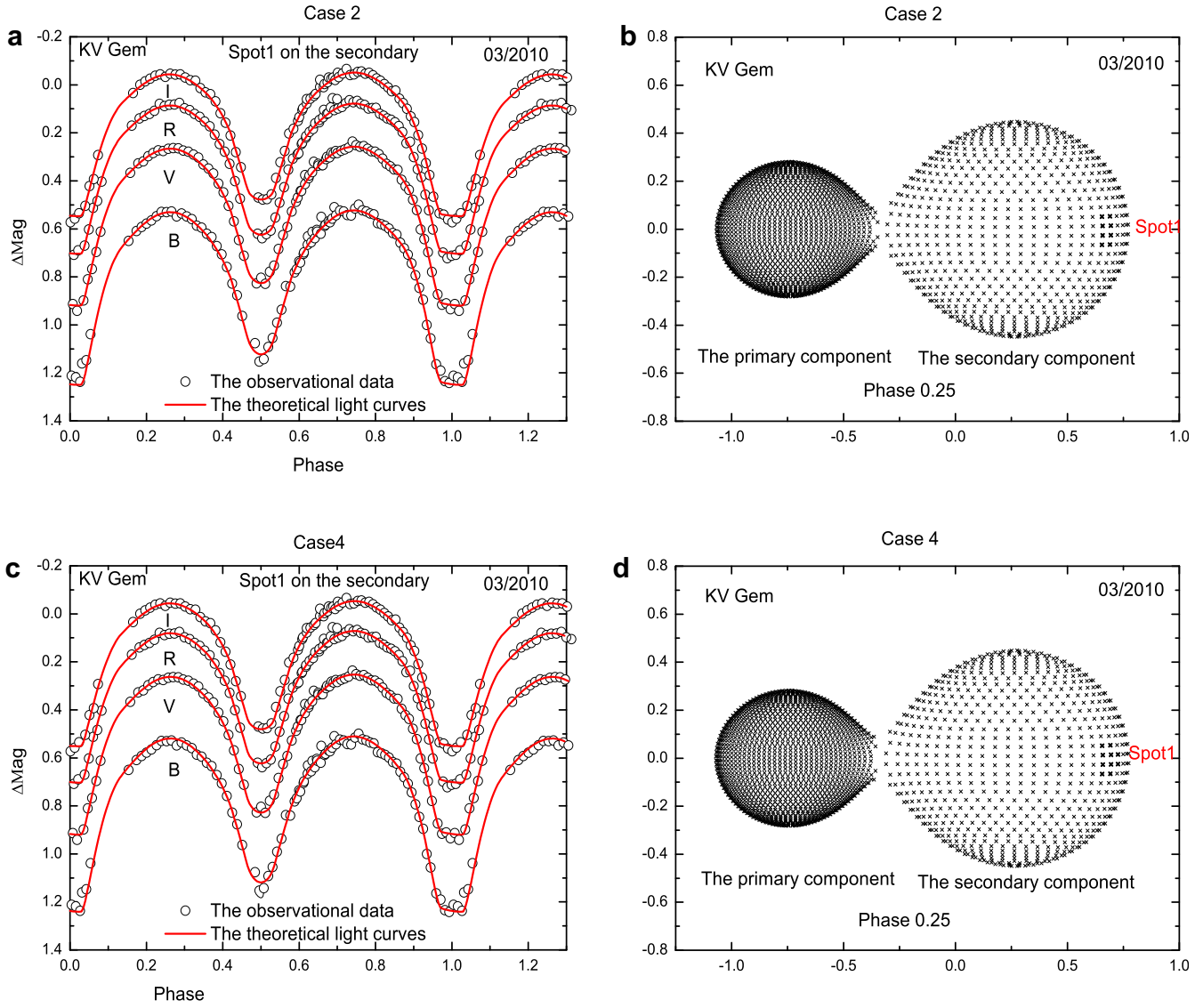

Fig. 7. The theoretical and observational light curves, and configuration of KV Gem in phase 0.25 in 2010 based on the photometric results of case 2 and case 4 of 2011.

temperature difference of about 300 K between the primary and secondary components and with a degree of contact factor $f = 24.6(\pm 0.8)\%$. With the orbital period decreasing, the inner and outer Roche lobes will shrink, causing the contact degree to increase.

The most reliable starspot parameters is active-region longitude by the traditional light curves method (Berdyugina, 2005). Comparing the starspot longitudes in different seasons (especially for March 2010 and November 2011) (See Tables 5 and 6). The starspot longitudes of KV Gem are variable on a long time scale of about one year. For the evaluation of the total distortion of the light curves, Pribulla et al. (2000) introduced a dimensionless factor β as the ratio between the luminosity blocked by spots and the total luminosity of an unspotted binary. We calculated them using the following function

$$\beta = \frac{\sum_{i=1}^{2}\sum_{j=1}^{n_1,n_2} r_i^2 sin^2(R_j/2)T_i^4(1-k_j^4)}{r_1^2T_1^4 + r_2^2T_2^4} \quad (5)$$

where n_1 spots are on primary and n_2 spots on secondary, T_1 and T_2 are the mean temperature of the unspotted components, k_j are the temperature factors and R_j are the radii of j-th spot and r_j are the radii of the components (Pribulla et al., 2000). The resulting spot factors are given in the Tables 5 and 6. The spot factors of KV Gem changed on the long time scale of several years. We found strong absorption in the observed H_β and H_γ lines, and Ca II H & K spectra, and no obvious emission in the subtracted spectra. This indicate that the chromospheric activity for KV Gem is very weak.

For KV Gem, it is one of the well observed systems and has been observed by the ASAS (Pojmanski, 2002, 2003; Pojmanski et al., 2005) for a long time. To discuss active evolution of KV Gem, we plotted the ASAS data in phases 0.0, 0.25, 0.5, and 0.75 in Fig. 10. For KV Gem, the brightness vary with time, which means that there is a possible photospheric active evolution. In order to confirm the possible active evolution, we used a simple function to fit, which are displayed by the dashed lines in Fig. 10. However, because the data is rather short about 6 years, it's too early to obtain the magnetic cycle. More data are needed to detect stellar cycle of KV Gem.

To clarify the period change, we firstly considered the possibility of orbital period variation. The (O–C) diagram suggests the decrease of period with the cyclic oscillation. The continuous period decrease rates are $dP/dt = 2.4(0.2)\times10^{-7}$ days/year for the polyno-

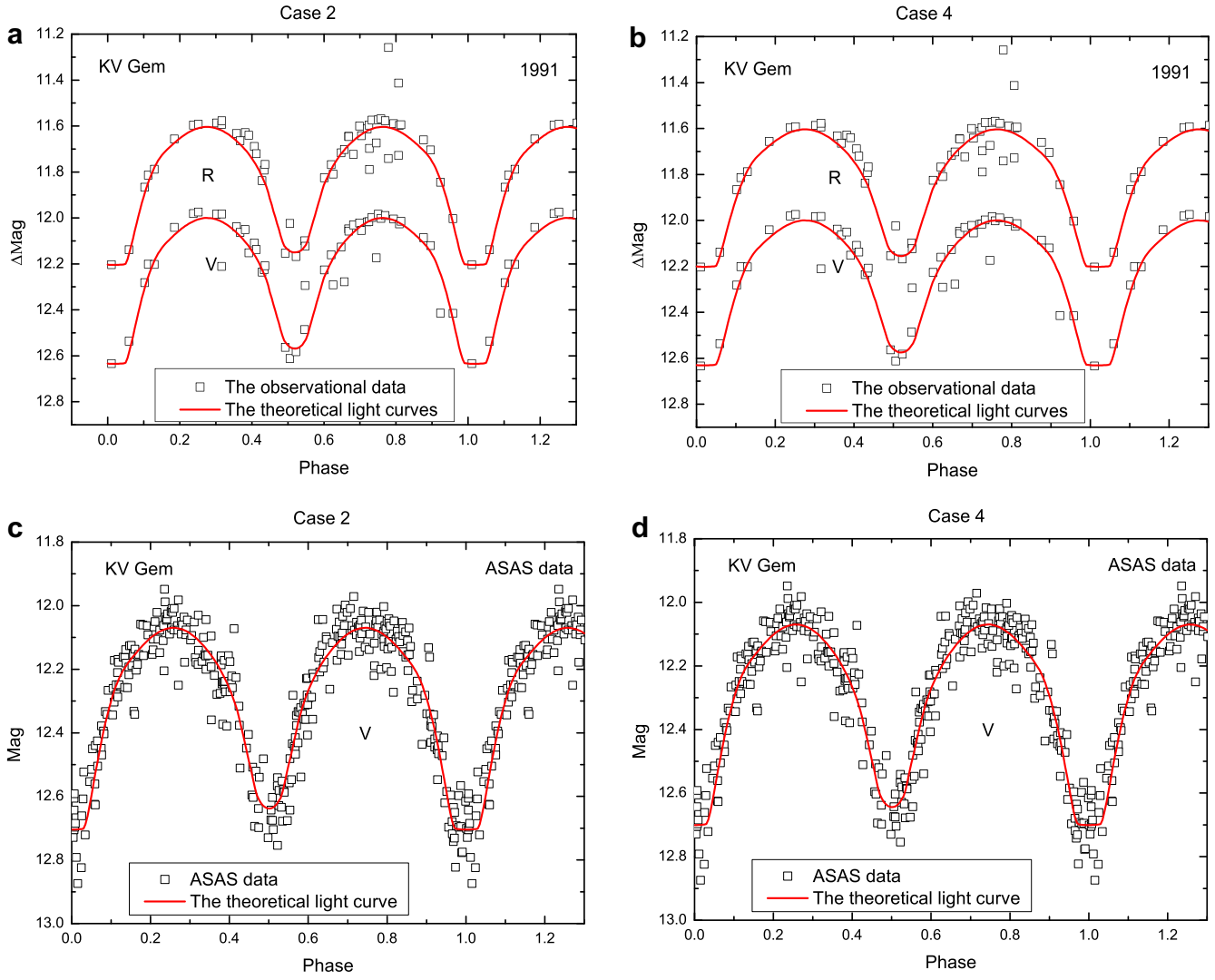

Fig. 8. The theoretical and observational light curves of 1991 and ASAS data based on the results of case 2 and case 4 of 2011.

mial and LITE function (Eq. 2) and $dP/dt=3.9(0.4)\times10^{-7}$ days/year for the polynomial and sine function (Eq. 4). Since KV Gem is a contact system, the secular period decrease might be caused by mass transfer from the more massive (Secondary) component to the less massive (primary) one. Using the following equation (Singh and Chaubey, 1986),

$$\frac{\dot{P}}{P} = 3\frac{\dot{M}_2}{M_2}\left(\frac{M_2}{M_1} - 1\right) \tag{6}$$

the mass transfer rates were estimated to be, $dM_2/dt = 3.4(0.3)\times10^{-7}$ $M_\odot$/year for Eq. 2 and $dM_2/dt = 5.5(0.6)\times10^{-7}$ $M_\odot$/year for Eq. (4), where the primary mass M_1 (0.98 $M_\odot$) were calculated by assuming that the primary component is a normal and main-sequence G0V star (Cox, 2000). The mass of the secondary component $M_2 = 2.74$ $M_\odot$ are calculated on the assumed primary mass and our obtained mass ratio. On the other hand, the period decrease might be due to magnetic braking (Applegate, 1992; Lanza et al., 1998; etc).

The oscillating characteristic may be caused by the light-time effect due to the existence of the third body (polynomial + LITE) or magnetic activity cycles of the system (polynomial + sine).

On one hand, the period oscillation may be explained by magnetic cycle (sine function). Spots in binary systems can cause asymmetries in the light curves that displace the observed time of minimum from the true time of minimum by up to 0.001–0.005 days (Pribulla et al., 2000; Coughlin et al., 2008, etc). The amplitude of the sine function of KV Gem is 0.0016 ± 0.0002. The amplitude of KV Gem is the same to the value of magnitude caused by starspot, and thus can be considered as a possibility of spot cycles. The period variation is $dP/dt = 1.1\times10^{-6}$ days/years ($dP/P = 3.1\times10^{-6}$ cycles/year). The size of the periodic variation $\Delta P/P = 3.1\times10^{-6}$ can be computed in days using the equation $\Delta P/P = A\times\sqrt{2[1-cos(2\pi\times P/T)]}/P$ (Rovithis-Livaniou et al., 2000), where A is the amplitude of the sine function, and T is the period of magnetic activity. The orbital period change corresponding to a variation of the quadrapole moment is given by $\Delta Q = -(\Delta p/p)\times(Ma^2/9)$ (Applegate, 1992) where a is the separation between the two components $a = 3.50$ $R_\odot$ (The separation between the two components of KV Gem was calculated based the assumed primary radius R_1 (1.06 $R_\odot$) according to spectral type and our photometric relative radius.) and M is the mass of the active component. Therefore, the quadrupole moment ΔQ_1 is calculated to be 1.9×10^{51} g cm^2 for the primary component and $\Delta Q_2 = 5.3\times10^{51}$ g cm^2 for the secondary component. The values of the quadrupole moment are similar to the typical values ($10^{51}-10^{52}$) of active binaries (Lanza and Rodonò, 1999).

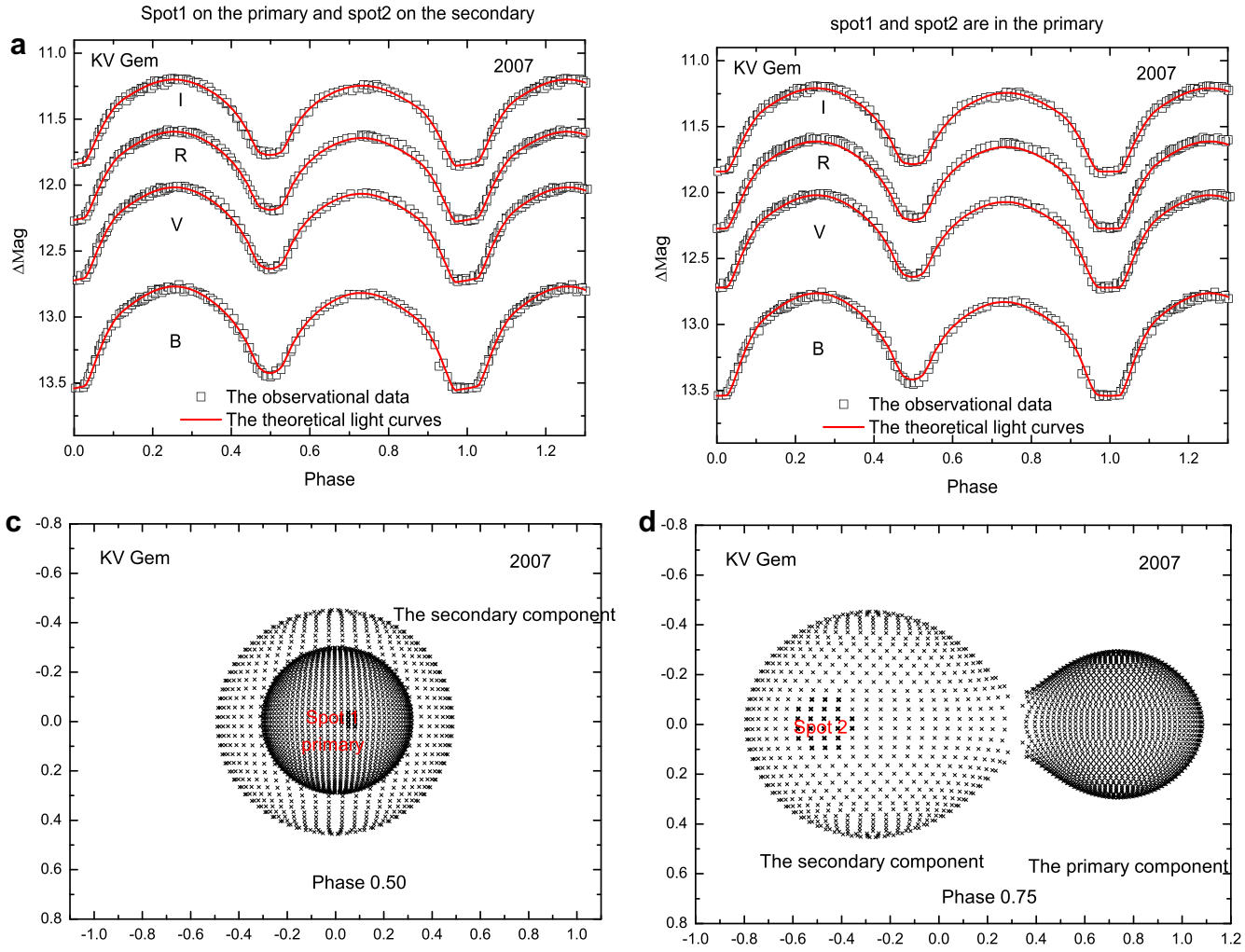

Fig. 9. The theoretical and observational light curves of the data published by Coughlin (2010), and their configurations for the better results of KV Gem in phase 0.5, and 0.75.

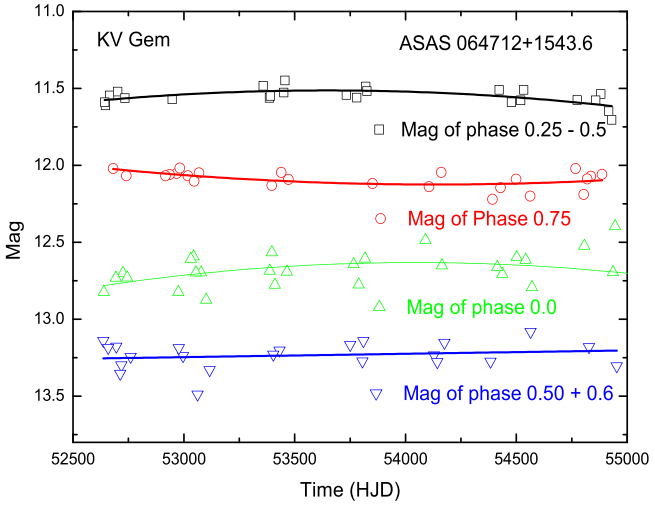

Fig. 10. The BVRI brightness of ASAS in phase 0.0, 0.25, 0.5 and 0.75 vs HJD.

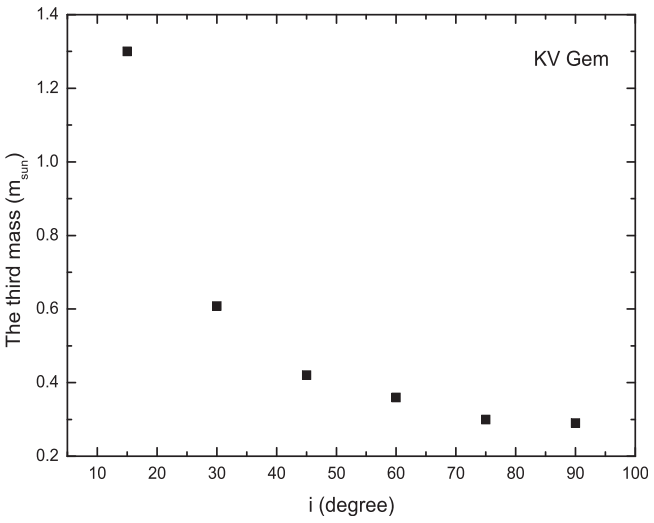

Fig. 11. Relations between the orbital inclination and the mass for the third body for KV Gem.

Therefore, the period oscillation may be accounted by magnetic cycle of the system (Applegate, 1992; Lanza et al., 1998; Lanza and Rodonò, 1999).

On the other hand, the period oscillation may be explained by the light-time effect of a third body. The semi-amplitudes K_{RV} of the changes of the systemic velocity accompanies by the light time effect is given by Mayer (1990),

Table 7
Physical parameters and orbital period nature for some binaries (the mass ratio is larger than 1).

Star name	Period	q	dp/dt	A	P_3	reference
uint	days		year	days	year	
V524 Mon	0.28362	2.1	−1.52E-10	0.0082	23.93	1
BE Cep	0.42439	2.34	−4.84E-08	0.0067	59.26	2
BX Peg	0.28042	2.34	−9.84E-08	0.0113	59.61	3
CW Cas	0.31886	2.23	−3.44E-08	0.0067	63.7	4
EH Cnc	0.41804	2.51	−1.01E-07	0.0032	16.6	5
VW boo	0.34232	2.336	−1.45E-07	0.0059	25.96	6
KV Gem	0.35852	2.8	−2.4or3.4E-7	0.0016/ 0.0029	8.8/ 10.3	7

1. He et al. (2012); 2. Dai et al. (2012); 3. Lee et al. (2009); 4. Jiang et al. (2010); 5. Yang et al. (2011); 6. Liu et al. (2011);7.my paper.

$$K_{RV} = \frac{2\pi}{P_3}\frac{a_{12}\sin i_3}{\sqrt{1-e^2}} \tag{7}$$

where K_{RV}, P_3, and a_{12} are in kilometers per second, years, and days, respectively. Using Eq. (7), the semi-amplitudes for the third body from Eq. (3) can be estimated to be 1.6 ± 0.2 km/s, respectively. The mass function ($f(M_3) = 0.0015(\pm 0.0003)\ M_\odot$) could be calculated by using the following equation:

$$f(m) = \frac{4\pi^2}{GT^2} \times (a'_{12}\sin i')^3 = \frac{(M_3 \sin i'_3)^3}{(M_1+M_2+M_3)^2}. \tag{8}$$

The mass of the third component can also be calculated with the above Eq. (8) and depends on the orbital inclination. The relation between the orbital inclination and the mass of the third body is displayed in Fig. 11. The minimal mass $M_{3,min}$ is 0.29 $M_\odot$ when $i' = 90^\circ$. According to Allen's stable (Cox, 2000), the spectral type for the assumed third body can be estimated to be a M3 – M4 star, which might be a dwarf. For this case, it is difficult to find a direct evidence of the third body by spectroscopic and photometric observation. If the additional tertiary component is true, KV gem might be a third system. Our result of KV Gem may further confirmed the hypothesis that most of contact binaries exist in multiple systems (Pribulla et al., 2000; Rucinski, 2007 ; etc). This kind of phenomenon of the period decrease and cyclic variation was also found in many other contact binaries with the mass ratio $\geqslant 1$ (see Table 7), which including their physical parameters (the period decrease rate and the amplitude and period of cyclic oscillation).

Acknowledgements

The authors would like to thank the observing assists of 85 cm telescope of Xinglong station for their help during our observations. We would also like to thank the anonymous referee for his (her) valuable comments, which led to large improvement in the manuscript. We also thank Coughlin, J. L and Schmidt, E.G for providing their data. This work is partly supported by GuiZhou University under Grant No. 2008036, GuiZhou natural Science Foundation No. 20092263 and supported partly by the Joint Fund of Astronomy of the National Natural Science Foundation of China (NSFC) and the Chinese Academy of Sciences (CAS) Grant Nos. 10978010, U1231102, 11203005 and 11263001. This work was partially Supported by the Open Project Program of the Key Laboratory of Optical Astronomy, NAOC, CAS. This research has made use of the Simbad database, operated at CDS, Strasbourg, France.

References

Achterberg Herbe, H., 2003. BAV 52, 93.
Agerer, f., Hübscher, J., 1996. IBVS 4382.
Agerer, F., Hübscher, J., 1998. IBVS 4562.
Agerer, Hübscher, 2002. IBVS 5296, 1.
Agerer, F., Hübscher, J., 2003. IBVS 5484.
Agerer, F., Dahm, M., Hübscher, J., 1999. IBVS 4712.
Applegate, J.H., 1992. ApJ 385, 621.
Barden, S.C., 1985. ApJ 295, 162.
Berdyugina, S.V., 2005. Living Rev. Solar Phys. 2, 8 (Online Article).
Bessell, M.S., Brett, J.M., 1988. PASP 100, 1134.
Brát, L., Zejda, M., Svoboda, P., 2007. OEJV 5964.
Brát, L., Trnka, J., Smelcer, L., et al., 2011. OEJV 137.
Coughlin, J.L., 2010. ARXIV 1004, 1395 [astro-ph.SR].
Coughlin, J.L., Dale III, H.A., Williamon, R.M., 2008. AJ 136, 1089.
Cox, A.N., 2000. In: Allen's Astrophysical Quantities, 4th ed. Springer, New York, p. 388.
Cutri, R.M., Skruskie, M.F., van Dyk, S., et al., 2003. yCat 2246, 0.
Dai, H.F., Yang, Y.G., Hu, S.M., et al., 2012. NewA 17, 347.
Davidge, T.J., Milone, E.F., 1984. Apjs 55, 571.
Diethelm, R., 2009. IBVS 5894.
Diethelm, R., 2010. IBVS 5945.
Diethelm, R., 2011. IBVS 5960.
Dvorak, S., 2006. IBVS 5677.
Eker, Z., Demircan, O., Bilir, S., Karatas, Y., 2007. ASPC 370, 151.
Fang, X.S., Gu, S.H., Cheung, S.L., et al., 2010. RAA 10, 253.
Flannery, B.P., 1976. ApJ 205, 208.
Gettel, S.J., Geske, M.T., McKay, T.A., 2006. AJ 131, 621.
Gunn, A.G., Doyle, J.G., 1997. A&A 318, 60.
He, J.J., Wang, J.J., Qian, S.B., 2012. PASJ 64, 85.
Hilditch, R.W., King, D.J., Mcfarlane, T.M., 1988. MNRAS 231, 341.
Hoffman, D.I., Harrison, T.E., McNamara, B.J., et al., 2006. AJ 132, 2260.
Hog, E., Fabricius, C., Makarov, V.V., et al., 2000. A&A 355, 27.
Hübscher, J., 1994. BAVSM 68.
Hübscher, J., 2005. IBVS 5643.
Hübscher, J., 2007. IBVS 5802.
Hübscher, J., 2011. IBVS 5984.
Hübscher, J., Monninger, G., 2011. IBVS 5959.
Hübscher, J., Walter, F., 2007. IBVS 5761.
Hübscher, J., Paschke, A., Walter, F., 2005. IBVS 5657.
Hübscher, J., Paschke, A., Walter, F., 2006. IBVS 5731.
Hübscher, J., Steinbach, H., Walter, F., 2009. IBVS 5874.
Hübscher, J., Steinbach, H., Walter, F., 2009b. IBVS 5889.
Hübscher, J., Steinbach, H., Walter, F., 2010a. IBVS 5918.
Hübscher, J., Lehmann, P.B., Monninger, G., et al., 2010b. IBVS 5941.
Jiang, T.Y., Li, L.F., Han, Z.W., et al. 2010. PASJ 62, 457.
Kallrath, J., Milone, E.F., 2009. Eclipsing Binary Stars: Modeling the Analysis. Astronomy and Astronphysics Library, Springer, Dordrecht Heidelberg London and New York.
Kaluzny, J., 1985. Acta Astron. 35, 327.
Kholopov, P.N., Samus, N.N., Kazarovets, E.V., 1985. IBVS 2681.
Kukarkin, B.V., Efremov, Y.N., Frolov, M.S., et al., 1968. IBVS 311.
Kurucz, R.L., 1993. In: Milone, E.F. (Ed.), Light Curve Modeling of Eclipsing Binary Stars. Springer-Verlag, New York, p. 93.
Kwee, K.K., van Woerden, H., 1956. BAN 12, 327.
Lanza, A.F., Rodonò, M., 1999. A&A 349, 887.
Lanza, A.F., Rodonò, M., Rosnor, R., 1998. MNRAS 296, 893.
Lee, J.W., Kim, S.L., Lee, C.U., et al., 2009. PASP 121, 1366.
Liu, L., Qian, S.B., Zhu, L.Y., et al., 2011. AJ 141.
Lucy, L.B., 1967. Z. Astrophys. 65, 89.
Lucy, L.B., 1976. ApJ 205, 217.
Mayer, P., 1990. BAICz 41, 231.
Montes, D., Fernández-Figueroa, M.J., De Castro, E., Cornide, M., 1995. A&A 294, 165.
Montes, D., Fernández-Figueroa, M.J., De Castro, E., Sanz-Forcada, J., 1997. A&AS 125, 263.
Montes, D., Crespo-chaón, I., Gálvez, M.C., et al., 2004. LNEA 1, 119.
Nelson, R.H. 2007. Software by Bob Nelson, http://members.shaw.co/bob.nelson/software1.htm
Paschke, A., Brat, L., 2006. OEJV 23, 13P.
Pojmanski, G., 2002. AcA 52, 397.
Pojmanski, G., 2003. AcA 53, 341.
Pojmanski, G., Pilecki, B., Szczygiel, D., 2005. AcA 55, 275.
Press, W., Teukolsky, S.A., Flannery, B.P., Vetterling, W.T., 1992. Numerical Recipes in Fortran. Cambridge Univ. Press.
Pribulla, T., Rucinski, S.M., 2006. AJ 131, 2986.
Pribulla, T., Chochol, D., Milano, L., et al., 2000. A&A 362, 169.
Qian, S.B., 2002. MNRAS 336, 1247.
Robertson, J.P., Eggleton, P.P., 1977. MNRAS 179, 359.
Rovithis-Livaniou, H., Kranidiotis, A.N., Rovithis, P., et al., 2000. A & A 354, 904.
Rucinski, S.M., 1973. Acta Astron. 23, 79.
Rucinski, S.M., Pribulla, T., van Kerkwijk, M.H., 2007. AJ 134, 2353.
Šafář, J., Zejda, M., 2000. IBVS 4888.
Šafář, J., Zejda, M., 2002. IBVS 5263.

Samus, N.N., Goranskii, V.P., Durlevich, O.V., et al., 2003. AstL 29, 468.
Schmidt, E.G., 1991. AJ 102, 1766.
Shaw, J.S., 1994. Mem. Soc. Astron. Ital. 65, 95.
Singh, M., Chaubey, U.S., 1986. Ap&SS 124, 389.
Stępień, K., 2006. AcA 56, 199.
Van Hamme, W., 1993. AJ 106, 209.
Wilson, R.E., 1990. ApJ 356, 613.
Wilson, R.E., 1994. PASP 106, 921.
Wilson, R.E., Devinney, E.J., 1971. ApJ 166, 605.
Wilson, R.E., Van Hamme, W. 2004. Computing Binary Star Observables, privately circulated monograph.
Yang, Y.G., Dai, J.M., Yin, X.G., 2007. AJ 134, 179.
Yang, Y.G., Shao, Z.Y., Pan, H.J., et al., 2011. PASP 123, 895.
Zeijda, M., 2002. IBVS 5287.
Zejda, M., 2004. IBVS 5583.
Zejda, M., Mikulásek, Z., Wolf, M., 2006. IBVS 5741.
Zhang, L.Y., 2010. PASP 122, 309.
Zhang, L.Y., 2011. ASPC 451, 123.
Zhang, L.Y., 2012. RAA 12, 433.
Zhang, L.Y., Gu, S.H., 2007. A&A 471, 219.
Zhang, L.Y., Zhang, X.L., Zhu, Z.Z., 2010a. NewA 15, 362.
Zhang, L.Y., Jing, J.H., Tang, Y.K., Zhang, X.L., 2010b. NewA 15, 653.
Zhou, A.Y., Jiang, X.J., Zhang, Y.P., et al., 2009. RAA 9, 349.
Zhu, L.Y., Qian, S.B., 2006. MNRAS 367, 423.